

# **AMCoR**

Asahikawa Medical College Repository <http://amcor.asahikawa-med.ac.jp/>

Physical Review B (2006) 73(15):155430.

Size-dependent change in energy bands of nanoparticles of white tin

Anno E, Tanimoto M

# Size-dependent change in energy bands of nanoparticles of white tin

E. Anno and M. Tanimoto

*Department of Physics, Asahikawa Medical College, Asahikawa, Hokkaido 078-8510, Japan*

(Received 7 December 2005; revised manuscript received 3 February 2006; published 26 April 2006)

For white-Sn particles smaller than about 500 Å in diameter, interband absorption, arising from transitions between nearly parallel bands, has been studied experimentally. In particle sizes smaller than about 300 Å in diameter, interband absorption appearing at about 3.1 and 3.8 eV is shifted to higher energies with decreasing particle size. In particle sizes smaller than about 100 Å in diameter, interband absorption appearing at about 5.0 eV is shifted to lower energies with decreasing particle size. The shift to the lower and higher energies can qualitatively be attributed to the energy-band narrowing by low coordination-number of surface atoms and to the energy-band broadening by lattice contraction, respectively. Thus, both the low coordination-number and the lattice contraction cause depending on size the change in energy bands. The interband absorption weakened with shifting and finally disappeared, indicating a decrease in the joint density of states. Thus, the initial and final bands are considered to depart from nearly parallel with energy-band narrowing and broadening.

DOI: 10.1103/PhysRevB.73.155430

PACS number(s): 78.66.Bz, 78.20.-e

## I. INTRODUCTION

Small particles are special states of matter intermediate between atoms and solids. Thus, energy bands of small particles are expected to be different from those of bulk and are fundamental interest in solid-state physics. If energy bands of small particles are affected by particle size, we can study the energy bands by analyzing the influence of particle size on interband absorption of the small particles.

In bulk metals, surface layers have narrower energy bands than bulk because coordination number is lower for surface atoms than for bulk atoms.<sup>1,2</sup> In metal particles, the ratio of surface to volume atoms increases with decreasing particle size, thereby strengthening the effect of low coordination-number of surface atoms on energy bands. Thus, energy bands of metal particles narrow as the particle size is decreased. An experimental study<sup>3</sup> of interband absorption of Pb particles has reported that the conduction-band narrowing is attended with the change in the distribution of the density of states of the conduction bands.

In bulk metals, contraction of lattice constants causes the broadening of energy bands.<sup>4</sup> Lattice constants of metal particles contract with decreasing particle size because of the hydrostatic pressure due to the particle surface stress.<sup>5</sup> Experimental studies<sup>6,7</sup> of interband absorption of noble and transition metal particles have showed that energy bands of metal particles broaden with lattice contraction.

By <sup>119</sup>Sn conversion electron Mössbauer spectroscopy, x-ray absorption spectroscopy, and transmission electron microscopy, Spiga *et al.*<sup>8</sup> have studied structural properties of white-Sn particles produced by ion implantation in thin SiO<sub>2</sub> film. They found lattice contraction and coordination-number reduction originating from low coordination number of surface atoms. Based on this finding, we predict for white-Sn particles that both the low coordination number and the lattice contraction influence energy bands. It would be interesting to study how the energy bands are influenced.

In the present study, by investigating size-dependent change in interband absorption of white-Sn particles, we

qualitatively discuss the energy-band change due to both the low coordination-number and the lattice contraction.

## II. EXPERIMENT

In a vacuum chamber, a fused-quartz substrate (18×18×0.5 mm<sup>3</sup>) and electron-microscopic meshes covered with a carbon film were adjacently placed above an evaporation source. The distance (30.3 cm) from the evaporation source to the substrate equaled that to the meshes. SiO<sub>2</sub> was first deposited both on the fused-quartz substrate and the meshes by electron beam heating in an oil-free vacuum of ~10<sup>-8</sup> Torr. Next, at pressures of ~10<sup>-7</sup> Torr, white Sn (purity 99.9999%) was deposited to obtain island films consisting of white-Sn particles. Then, the island films were annealed for 1 h. The substrate and meshes were maintained at a temperature of about 333 K during deposition and annealing. After annealing, the films were coated with SiO<sub>2</sub> (thickness 100–300 Å) to prevent adsorption or chemical reactions on exposure to air. The weight thickness and the deposition rate were monitored with a quartz-crystal oscillator. Transmittance of the evaporated SiO<sub>2</sub> film was almost constant within the spectral range of interest here.

Optical and electron-microscopic investigations were carried out after exposing the samples to air. With a double-beam spectrophotometer (Shimadzu UV-365), transmittance spectra for normal incidence and their first derivatives were measured in the wavelength range of 190–2500 nm at room temperature within the experimental accuracy of ±0.1% and ±[0.3 (190 nm)–0.7 (2500 nm)] nm. The first-derivative spectra were derived by computer applications based on the convolution method for a wavelength interval of about 4 nm. The particle size and electron-diffraction pattern were investigated with an electron microscope operating at 200 kV (Hitachi H-800). For simplicity, we assumed the particle shape, difficult to observe three dimensionally, to be spherical and estimated the particle diameter by regarding the length around the outside of the particle as the circumference. The particle size distribution was evaluated as vol. %.

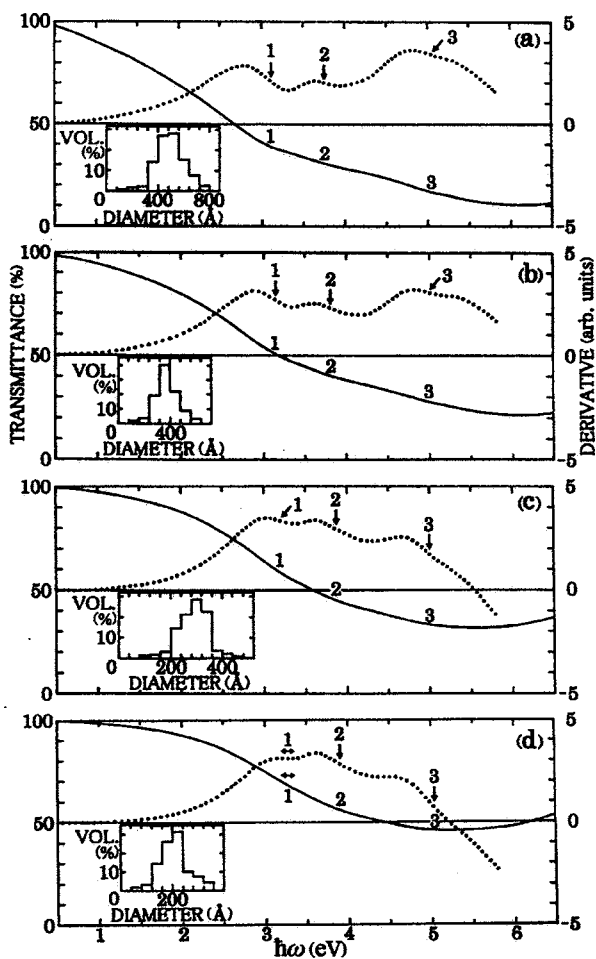


FIG. 1. Transmittance spectra (solid curves) and the first derivatives (dotted curves) of white-Sn island films with particle diameters of about (a) 480, (b) 360, (c) 300, and (d) 200 Å. The weight thickness is (a) 110.6, (b) 77.4, (c) 55.3, and (d) 38.7 Å. The deposition rate was (a) 0.18, (b) 0.18, (c) 0.18, and (d) 0.19 Å/s.

III. RESULTS

In Figs. 1 and 2, we show the transmittance and the first-derivative spectra compactly, by converting the wavelength unit (nm, Sec. II) into the photon energy unit (eV). Due to the conversion, the slope sign of the first derivative is reverse. In derivative spectroscopy,<sup>9</sup> the location of the maximum slope in a step appearing in the first derivative corresponds to that of absorption. In Figs. 1 and 2, the arrow indicates the location of the maximum slope in the step, and in the transmittance spectrum this location is labeled with a number as the location of absorption.

The location of absorption is expressed below by  $E \pm \Delta E$ , which shows that the slope is at its maximum in the range of  $(E - \Delta E) - (E + \Delta E)$ . Figures 1(a)–1(d) show the transmittance spectra and their first derivatives of the white-Sn island films with particle diameters of about 480, 360, 300, and 200 Å, respectively. The location of absorption 1 is (a)  $3.12 \pm 0.03$  eV, (b)  $3.14 \pm 0.03$  eV, and (c)  $3.19 \pm 0.03$  eV. It was difficult to identify the location of absorption 1 in Fig. 1(d), because the step for this absorption is ill defined in the derivative. Thus, we represent the range of presence

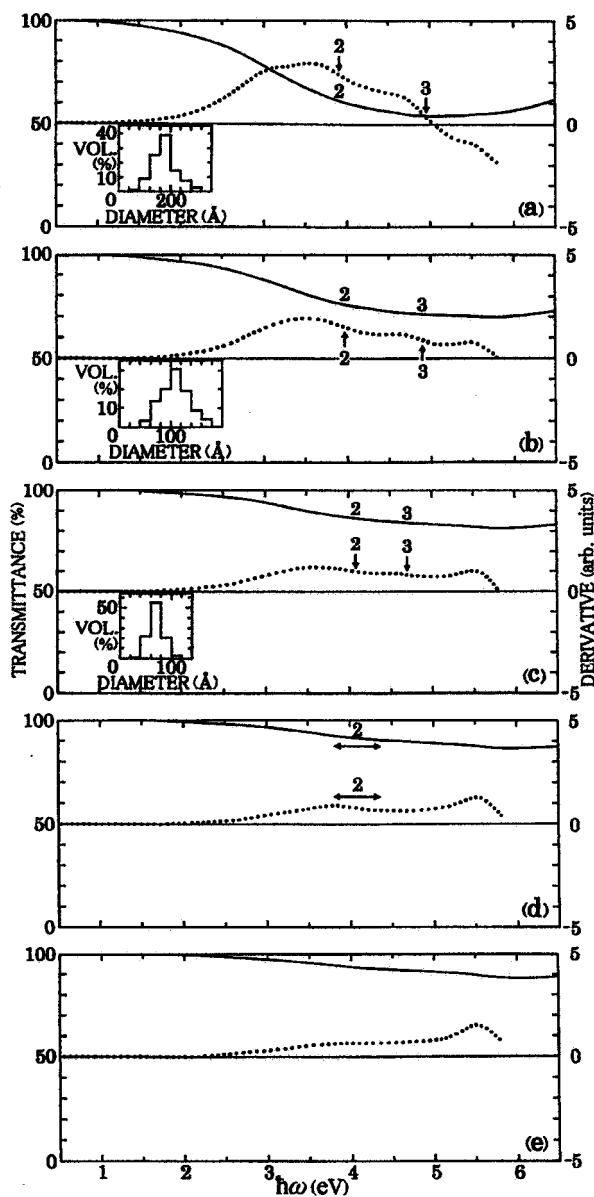


FIG. 2. Transmittance spectra (solid curves) and the first derivatives (dotted curves) of white-Sn island films with particle diameters of about (a) 180, (b) 110, and (c) 70 Å in diameter. Particle sizes for the films of (d) and (e) were difficult to investigate. The weight thickness is (a) 33.2, (b) 22.1, (c) 11.1, (d) 7.7, and (e) 5.5 Å. The deposition rate was (a) 0.17, (b) 0.18, (c) 0.18, (d) 0.19, and (e) 0.23 Å/s.

(3.19–3.35 eV) by a double-ended horizontal arrow. The location of absorption 2 is (a)  $3.75 \pm 0.04$  eV, (b)  $3.81 \pm 0.06$  eV, (c)  $3.87 \pm 0.05$  eV, and (d)  $3.90 \pm 0.05$  eV. Absorption 3 is located at (a)  $5.04 \pm 0.12$  eV, (b)  $4.98 \pm 0.06$  eV, (c)  $5.00 \pm 0.08$  eV, and (d)  $5.04 \pm 0.08$  eV.

We see in transmittance spectra in Fig. 1 that in addition absorption 1–3 there is absorption in the range above about 5.5 eV. The step for the absorption is incomplete in derivative spectra, so that the analysis based on the derivative was difficult for the absorption. For this reason, we did not investigate the absorption.

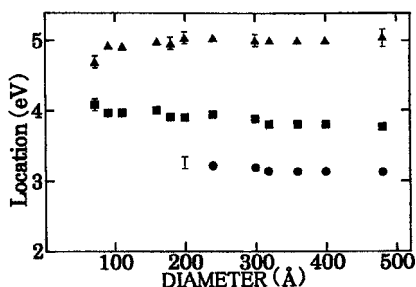


FIG. 3. The locations of interband absorption 1–3 plotted against particle diameter. ● interband absorption 1; ■ interband absorption 2; ▲ interband absorption 3. The bar at 200 Å in diameter for interband absorption 1 corresponds to the double-ended horizontal arrow in Fig. 1(d).

Metal island films consisting of metal particles smaller than the wavelength of incident light show interband absorption and/or optical plasma-resonance absorption due to plasma oscillations of conduction electrons in the metal particles.<sup>10</sup> Optical plasma-resonance absorption remarkably shifts to higher energies with decreasing weight thickness because of the decrease in the effective depolarization factor.<sup>10</sup> This shift was found, for example, for Al and In island films.<sup>11,12</sup> The decrease in the weight thickness from the film in Fig. 1(a) to the film in Fig. 1(d) is large (the decrease of about 65%), but the remarkable shift of absorption to higher energies is not found in Fig. 1. Thus, absorption 1–3 is not optical plasma-resonance absorption but interband absorption. In the following, absorption 1–3 is referred to as interband absorption 1–3, respectively.

The transmittance spectra and their first derivatives of the white-Sn island films with particle diameters of about 180, 110, and 70 Å are shown in Figs. 2(a)–2(c), respectively. The location of interband absorption 2 is (a)  $3.91 \pm 0.06$  eV (b)  $3.97 \pm 0.07$  eV, and (c)  $4.08 \pm 0.08$  eV. Interband absorption 3 is located at (a)  $4.96 \pm 0.08$  eV (b)  $4.90 \pm 0.06$  eV, and (c)  $4.69 \pm 0.07$  eV. Particle sizes for the films of Figs. 2(d) and 2(e) were difficult to investigate because of the low contrast due to the SiO<sub>2</sub> coating. The particle size for the film of Fig. 2(d) must be smaller than that of Fig. 2(c) and the particle size for the film of Fig. 2(e) must be smaller than that of Fig. 2(d), because the particle size decreases with decreasing weight thickness.<sup>13</sup> In Fig. 2(d), the maximum slope was difficult to distinguish in the step for interband absorption 2. Thus, the range of presence (3.80–4.36 eV) of this absorption is represented in a double-ended horizontal arrow.

Figure 3 shows the locations of interband absorption 1–3 plotted against particle diameter. The locations for films with particle diameters of about 400, 320, 240, 160, and 90 Å were also plotted, though spectra are not given in the present paper. If energy bands of white-Sn particles are the same as those of bulk, the locations of interband absorption 1–3 must be independent of particle size. In Fig. 3, in particle sizes larger than about 320 Å in diameter the locations of interband absorption 1–3 are almost independent of particle size. Thus, white-Sn particles, larger than this size, have energy bands the same as those of bulk. This is the case for particles in the films of Figs. 1(a) and 1(b), i.e., these figures show the spectra of bulk.

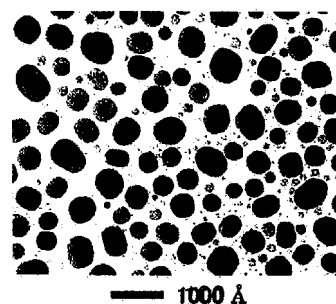


FIG. 4. Electron micrograph for the white-Sn island films with particle diameter of about 480 Å [Fig. 1(a)].

Figure 4 shows an electron micrograph of white-Sn island film with particle diameter of about 480 Å [Fig. 1(a)]. The particles display a complex contrast structure due to the diffraction contrast.<sup>14</sup> Thus, they are in a polycrystalline state, which is optically isotropic.

For films with particle diameters larger than about 160 Å, only a body-centered-tetragonal (bct) structure could always be identified in electron-diffraction patterns, implying that the formation of compound layers on the particle surface or the change of particles into compounds occurred rarely. From the (200) diffraction ring, it was found that the lattice constant  $a$  for particle sizes of about 300 and 160 Å in diameter is, respectively, about 0.6 and 1.6 % smaller than that of about 480 Å in diameter [Fig. 1(a)] (i.e., smaller than that of bulk). This shows contraction of lattice constants, confirming the occurrence of lattice contraction reported by Spiga *et al.*<sup>8</sup> (about 3% for the particles of 74 and 109 Å in diameter).

Electron-diffraction pattern was difficult to observe for Sn particles smaller than about 160 Å in diameter [Figs. 2(b)–2(e)] because of the low contrast due to the SiO<sub>2</sub> coating, so that we were not able to identify the crystal structure. In the study by Spiga *et al.*<sup>8</sup> Sn particles of 74 Å in diameter, comparable to the size (about 70 Å in diameter) in Fig. 2(c), have the bct structure. Thus, we consider Sn particles in the films of Figs. 2(b) and 2(c) to have the bct structure. It has been reported<sup>15</sup> that Sn particles smaller than about 50 Å in diameter have a specific phase between the liquid and the solid phase. If Sn particles have such phase, optical absorption must be entirely different from that of white-Sn particles. Absorption in the range above about 5.5 eV in Figs. 1 and 2(a)–2(c) is found also in Figs. 2(d) and 2(e). From this, Sn particles in the films of Figs. 2(d) and 2(e) presumably also have the bct structure.

## IV. DISCUSSION

### A. Comparison with previous data

There have been several studies of the optical absorption of bulk white-Sn (crystals or continuous films produced by vacuum evaporation). However, the absorption in the studies is different, for example, as follows. Based on an analysis of optical data of continuous films in the range 0.1–27.5 eV, MacRae *et al.*<sup>16</sup> have reported that interband absorption is present at 1.2, 3, and 24.5 eV. Schwarz<sup>17</sup> has measured on

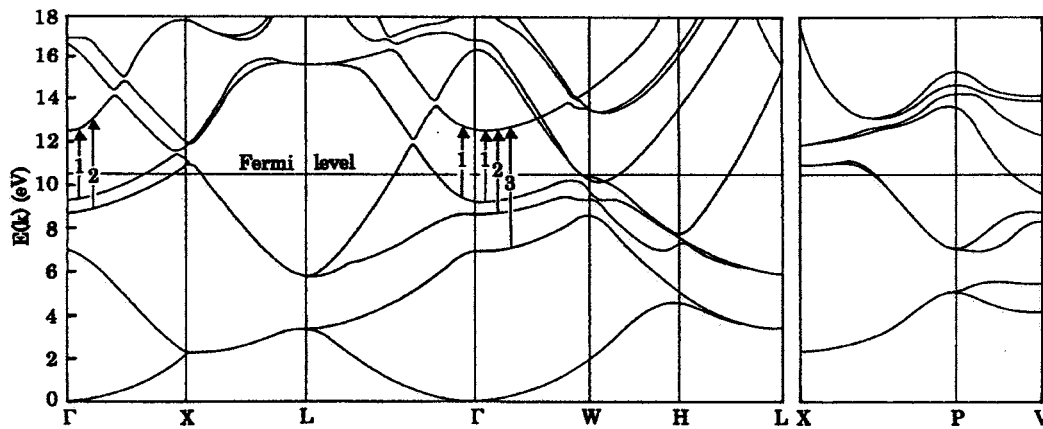


FIG. 5. Band structure of bulk white-Sn by Craven (Ref. 19). Transitions represented in arrows 1–3 correspond to interband absorption 1–3, respectively.

single crystals and continuous films in the 0.5–5.5 eV range. He reported that for polarization parallel to the tetragonal axis interband absorption exists at 1.15, 1.3, 3.4, and 4.1 eV, and in the range 1.6–4 eV, and that for polarization perpendicular to the tetragonal axis at 1.15, 1.3, 3.65, 4.2, and 4.7 eV. Jézéquel *et al.*<sup>18</sup> have measured on continuous films in the range from 2 to 15 eV and reported that interband absorption is found at 2, 3.6, 4.3, and 5.2 eV. We were not able to confirm the absorption in these studies because continuous films were difficult to produce in the present study.

Absorption in Figs. 1(a) and 1(b), correspond to absorption of bulk (Sec. III), is different from that in previous studies.<sup>16–18</sup> The cause of the difference was difficult to clarify. Possible causes are mentioned below. Interband absorption in the range below about 3 eV in the previous studies<sup>16,17</sup> could not be detected in the present study [Figs. 1(a) and 1(b)]. The reason may be that such interband absorption is very weak and thus difficult to detect because of the overlap with interband absorption 1–3. In the case of In particles,<sup>12</sup> weak interband absorption at about 1.4 eV (885 nm) was difficult to detect. Electron-diffraction patterns of compounds were not found for samples in the present study (Sec. III). The presence of compound layers on the sample surface was not checked in the previous studies.<sup>16–18</sup> The difference in absorption in the range above about 3 eV between the previous and present studies may be due to the presence of compound layers on the sample surface in the previous studies.

### B. Identification of transitions in energy bands

We reproduce the band structure of bulk white-Sn by Craven<sup>19</sup> in Fig. 5. The symmetry points are shown, but we have omitted the usual notation of the different bands and simply denote the first seven bands of interest as the first to seventh bands in order of increasing energy. Several bands are seen to be nearly parallel. As is well known, interband transition tends to occur strongly between parallel bands because the joint density of states (JDOS) is high.<sup>20</sup> Based on the Craven's band structure, Schwartz<sup>17</sup> has related observed absorption to transitions between nearly parallel bands along

some directions (such as  $\Gamma X$ ,  $\Gamma L$ ,  $\Gamma W$ , and  $PV$  directions). However, several discrepancies were found in the relation.

In the following, by comparing the locations of interband absorption 1–3 in Fig. 1(a) with energy differences between nearly parallel bands in the Craven's band structure, we ascribe interband absorption 1–3 to transitions between the nearly parallel bands. Island films in the present study consist of polycrystalline particles randomly oriented (Sec. III). Thus, we consider here all possible transitions, independently from the selection rules associated with different light polarization states.<sup>17</sup>

We identify interband absorption 1 with transitions from the fourth band to the fifth band along  $\Gamma X$ ,  $\Gamma L$ , and  $\Gamma W$  near  $\Gamma$  (arrow 1 in Fig. 5). This is because the location ( $3.12 \pm 0.03$  eV) of interband absorption 1 in Fig. 1(a) is almost in agreement with the energy difference (about 3.3–3.4 eV) between these bands.

The location ( $3.75 \pm 0.04$  eV) of interband absorption 2 in Fig. 1(a) agrees well with the energy difference (about 3.8–3.9 eV) between the third band and the fifth band along  $\Gamma X$  and  $\Gamma W$  near  $\Gamma$ . Thus, we relate interband absorption 2 to transitions between these bands (arrow 2 in Fig. 5).

The band structure in Fig. 5 gives an energy difference of about 5.7 eV between the second band and the fifth band along  $\Gamma W$  near  $\Gamma$ . This difference is comparable to the location ( $5.04 \pm 0.12$  eV) of interband absorption 3 in Fig. 1(a). Thus, transitions between these bands (arrow 3 in Fig. 5) are considered to be responsible for interband absorption 3.

The correspondence of the locations of interband absorption 1–3 to the energy differences in the band structure by Craven is good as mentioned above. Based on this, we consider that the Craven's band structure and interband absorption 1–3 are valid. Ament and Vroomen<sup>21</sup> have also calculated band structure of bulk white-Sn. However, there is poor correspondence with interband absorption in the present study.

### C. Size-dependent change in energy bands

Very little data on energy bands of surface layers of bulk white-Sn has been reported, and there has been very little

data on the effect of lattice contraction on energy bands of bulk white-Sn.

In Fig. 3, the location of interband absorption 3 is almost independent of particle size down to about 160 Å in diameter. From this fact, we consider the initial and final bands (the second and fifth bands) not to be shifted down to this size. The position of the fifth band, the final band common to interband absorption 1–3 (Fig. 5), was difficult to study for particle sizes smaller than about 160 Å in diameter. We assume here that the fifth band is not shifted also in particle sizes smaller than about 160 Å in diameter.

Energy bands of metal particles narrow as the effect of low coordination-number of surface atoms strengthens (Sec. I). In the narrowing, the positions of bands below Fermi level are raised relative to the Fermi level (the lower the positions, the larger the raising).<sup>22</sup> When energy spacing between the initial and final bands is decreased due to the raising of the position of the initial band, interband absorption shifts to lower energies. Spiga *et al.*<sup>8</sup> have found the coordination-number reduction (from 6 to around 5), originates from low coordination-number of surface atoms, for white-Sn particles of 74 and 109 Å in diameter. From this size, the effect of low coordination-number of surface atoms may appear for particle sizes smaller than about 100 Å in diameter. In Fig. 3, in particle sizes smaller than about 100 Å in diameter, interband absorption 3 is shifted to lower energies with decreasing particle size. Thus, the shift can qualitatively be ascribed to the energy-band narrowing. In this case, corresponding to the shift of the location of interband absorption 3 in Fig. 3, the initial band (the second band) is shifted to higher positions relative to the Fermi level.

Energy bands of metal particles broaden with lattice contraction (Sec. I). With broadening, interband absorption shifts to higher energies because energy spacing between the initial and final bands is increased.<sup>6,7</sup> In this increase, the position of the initial band is lowered relative to Fermi level. In the present study, lattice contraction was found for particle sizes of about 300 Å in diameter (Sec. III), and in particle sizes smaller than about 300 Å in diameter interband absorption 1 and 2 are shifted to higher energies with decreasing particle size (Fig. 3). Thus, we can qualitatively attribute the shift to the energy-band broadening. In this case, corresponding to the shift of the locations of interband absorption 1 and 2 in Fig. 3, the initial bands (the third and fourth bands) are shifted to lower positions relative to the Fermi level.

From this discussion of the shift of bands, we point out that in white-Sn particles both the low coordination number of surface atoms and the lattice contraction cause the change in energy bands. Presumably, there occurs the competition between the energy-band narrowing based on the low coordination number and the energy-band broadening based on the lattice contraction. As mentioned above, the narrowing and the broadening mainly appear for the second band and the third and fourth bands, respectively. This appearance seems to be the result of the competition, which was difficult to analyze in the present study.

The third and fourth bands, originate from the spin-orbit splitting,<sup>19</sup> are close to each other (Fig. 5). Therefore, we expect that these bands shift almost at the same time in lattice contraction, i.e., interband absorption 1 and 2 is expected

to shift almost at the same time. In Fig. 3, interband absorption 1 and 2 are shifted almost at the same time in particle sizes smaller than about 300 Å in diameter. This supports that the Craven's band structure<sup>19</sup> and interband absorption in the present study are valid.

Energy spacing between the second and third bands along  $\Gamma W$  near  $\Gamma$  almost equals the difference in the location between interband absorption 2 and 3 (Fig. 5). We see in Fig. 3 that this energy spacing is reduced from about 1.3 eV for bulk (i.e., for sizes larger than about 320 Å in diameter) to about 0.6 eV for particle sizes of about 70 Å in diameter.

In parallel bands,<sup>20</sup> if bands depart from parallel, interband absorption should weaken because the JDOS decreases with departure. Interband absorption should disappear when the decrease in the JDOS is large. In the present study, we regard interband absorption to disappear when the step for the interband absorption disappears in the derivative spectrum. In Figs. 1 and 2, the steps for interband absorption 1–3 become less and less defined with shift of their locations and finally disappear. That is, interband absorption 1–3 weakens with shifting and finally disappears, indicating a decrease in the JDOS. Therefore, we consider that the initial bands (the second, third, and fourth bands) and the final band (the fifth band) depart from nearly parallel with energy-band narrowing and broadening. It was difficult to clarify the mechanism of the departure.

The decrease in the JDOS for interband absorption 1–3 was difficult to investigate quantitatively. The particle size, below which interband absorption 1–3 disappears, is different as shown in Figs. 1 and 2. It was difficult to clarify the reason for this difference.

Optical constants of bulk white-Sn are uncertain at present because as mentioned in Sec. IV A absorption of bulk white-Sn in previous studies is different. For this, comparison with simulated spectrum based on bulk optical constants in the previous studies was not done in the present study.

#### D. Interactions with SiO<sub>2</sub>

The final band (the fifth band) is common to interband absorption 1–3 (Fig. 5). If electrons of the SiO<sub>2</sub> matrix occupy the final state in the final band, transitions would be restricted and thus interband absorption 1–3 would weaken or disappear at the same time. As shown in Figs. 1 and 2, when the particle size is decreased, interband absorption 1–3 did not disappear at the same time. This shows that the weakening and disappearance of interband absorption 1–3 are not due to occupation of the final state.

#### V. SUMMARY

We studied the interband absorption, due to transitions between nearly parallel bands, of white-Sn particles experimentally. In particle sizes smaller than about 300 Å in diameter, interband absorption at about 3.1 and 3.8 eV was shifted to higher energies with decreasing particle size. On the other hand, in particle sizes smaller than about 100 Å in diameter, interband absorption at about 5.0 eV was shifted to lower

energies with decreasing particle size. The shift to the lower and higher energies could qualitatively be explained by energy-band narrowing due to the low coordination number of surface atoms and by energy-band broadening due to the lattice contraction, respectively. It was thus pointed out that in white-Sn particles both the low coordination number and the lattice contraction cause the change in energy bands. The competition between the energy-band narrowing and broadening occurs, presumably. However, this point was difficult to investigate. The interband absorption weakened with shifting and finally disappeared, which shows a decrease in the

JDOS. From this, we considered that the initial and final bands depart from nearly parallel with energy-band narrowing and broadening. The mechanism of the departure was difficult to clarify.

#### ACKNOWLEDGMENTS

We are grateful to Masayuki Ido (Hokkaido University) for his encouragement throughout this work and valuable comments. One of us (E.A.) thanks Tomuo Yamaguchi (Shizuoka University) for his informative discussions.

- 
- <sup>1</sup>J. R. Smith, J. G. Gay, and F. J. Arlinghaus, *Phys. Rev. B* **21**, 2201 (1980).
- <sup>2</sup>J. Tersoff and L. M. Falicov, *Phys. Rev. B* **26**, 6186 (1982).
- <sup>3</sup>E. Anno and M. Tanimoto, *Phys. Rev. B* **66**, 165442 (2002).
- <sup>4</sup>See, for example, Y. Kubo and J. Yamashita, *J. Phys. F: Met. Phys.* **16**, 2017 (1986).
- <sup>5</sup>See, for example, R. Lamber, S. Wetjen, and N. I. Jaeger, *Phys. Rev. B* **51**, 10968 (1995), and references therein.
- <sup>6</sup>E. Anno, *Surf. Sci.* **260**, 245 (1992).
- <sup>7</sup>E. Anno and T. Yamaguchi, *Phys. Rev. B* **55**, 4783 (1997); E. Anno, *J. Appl. Phys.* **85**, 887 (1999).
- <sup>8</sup>S. Spiga, R. Mantovan, M. Fanciulli, N. Ferretti, F. Boscherini, F. d'Acapito, B. Schmidt, R. Grötzschel, and A. Mücklich, *Phys. Rev. B* **68**, 205419 (2003). In this reference, lattice contraction and coordination-number reduction have been studied only for white-Sn particles with diameters of 74 and 109 Å.
- <sup>9</sup>M. Cardona, *Modulation Spectroscopy* (Academic, New York, 1969), pp. 105–115.
- <sup>10</sup>See, for example, S. Norrman, T. Andersson, C. G. Granqvist, and O. Hunderi, *Phys. Rev. B* **18**, 674 (1978), and references therein.
- <sup>11</sup>H. V. Nguyen, I. An, and R. W. Collins, *Phys. Rev. B* **47**, 3947 (1993).
- <sup>12</sup>E. Anno and M. Tanimoto, *J. Appl. Phys.* **98**, 053510 (2005).
- <sup>13</sup>D. W. Pashley, M. J. Stowell, M. H. Jacobs, and T. J. Law, *Philos. Mag.* **10**, 127 (1964).
- <sup>14</sup>U. Kreibitz, *Z. Phys. B* **31**, 39 (1978); E. Anno and R. Hoshino, *J. Phys. Soc. Jpn.* **50**, 1209 (1981).
- <sup>15</sup>Y. Oshima and K. Takayanagi, *Z. Phys. D: At., Mol. Clusters* **27**, 287 (1993).
- <sup>16</sup>R. A. MacRae, E. T. Arakawa, and M. W. Williams, *Phys. Rev.* **162**, 615 (1967).
- <sup>17</sup>H. Schwarz, *Phys. Status Solidi B* **44**, 603 (1971).
- <sup>18</sup>G. Jézéquel, J. C. Lemonnier, and J. Thomas, *J. Phys. F: Met. Phys.* **7**, 2613 (1977).
- <sup>19</sup>J. E. Craven, *Phys. Rev.* **182**, 693 (1969).
- <sup>20</sup>See, for example, *Optical Properties of Solids*, edited by F. Abelès (North-Holland, Amsterdam, 1972), Chap. 4, Sec. 3.1.3.
- <sup>21</sup>M. A. E. A. Ament and A. R. de Vroomen, *J. Phys. F: Met. Phys.* **5**, 2394 (1975).
- <sup>22</sup>See, for example, R. P. Messmer, S. K. Knudson, K. H. Johnson, J. B. Diamond, and C. Y. Yang, *Phys. Rev. B* **13**, 1396 (1976).